

NATIONAL ADVISORY COMMITTEE FOR AERONAUTICS

RESEARCH MEMORANDUM

FLIGHT INVESTIGATION TO DETERMINE THE AERODYNAMIC
CHARACTERISTICS OF ROCKET-POWERED MODELS REPRESENTATIVE OF
A FIGHTER-TYPE AIRPLANE CONFIGURATION INCORPORATING
AN INVERSE-TAPER WING AND A VEE TAIL

By Sidney R. Alexander

SUMMARY

Two rocket-powered models representative of a fighter-type airplane were investigated in flight at Mach numbers up to 1.01 and 1.07 by the Langley Pilotless Aircraft Research Division at its testing station at Wallops Island, Va. These models incorporated an inverse-taper wing and a vee tail and were flown with controls undeflected and wing and stabilizer set at 0° incidence. Values of lateral acceleration, normal acceleration, velocity, and drag were obtained by use of telemeters and a Doppler velocimeter radar unit.

The results of this investigation indicated no unusual variation in the lateral acceleration characteristics. After the cessation of powered flight, the lateral oscillation quickly damped to zero. The data indicated that the airplane, at low lift coefficients, should not experience any abrupt trim changes until it attains a Mach number of 0.97. The change in normal-force coefficient associated with this trim change will amount to about 0.03 with the center of gravity located at 4.48 percent of the mean aerodynamic chord. At higher lift coefficients, on the basis of other data, the Mach number at which this trim change occurs would be expected to be decreased. The neutral point of the model at Mach numbers near 1.05 was estimated to fall at 45 percent of the mean aerodynamic chord, assuming a lift-curve slope of 0.05. A value of the static-directional-stability parameter $\frac{dC_n}{d\psi}$ of approximately -0.002 was estimated for a Mach number of 0.93. The values of drag coefficient obtained from both model flights were in a good comparative agreement. The highest drag coefficient occurred at a Mach number of 1.01 and was equal to 0.044.

INTRODUCTION

The Langley Pilotless Aircraft Research Division has conducted an investigation of rocket-powered models representative of a fighter-type

airplane configuration at its testing station, Wallops Island, Va. There are presented herein results obtained from flights of two vee-tail models having a tail length of 1.56 mean aerodynamic chords (measured from the quarter chord of the wing mean aerodynamic chord to the quarter chord of the tail mean aerodynamic chord) and controls undeflected. These results consist of lateral-force, normal-force, drag, and velocity data.

To avoid confusion, the two models tested will be designated "B" and "C" models.

SYMBOLS

t	flight time, seconds
M	flight Mach number (V/c)
V	flight velocity, feet per second
c	speed of sound, feet per second
W	weight of model, pounds
q	free-stream dynamic pressure, pounds per square foot $\left(\frac{\rho V^2}{2}\right)$
ρ	air density as determined from radiosonde observations, slugs per cubic foot
a	resultant acceleration along the flight path, feet per second per second
a_y	lateral acceleration, feet per second per second
a_n	normal acceleration, feet per second per second
g	acceleration due to gravity, 32.2 feet per second per second
S	total wing area, square feet
C_D	drag coefficient $\left(\frac{\text{Drag}}{qS}\right)$
C_N	normal-force coefficient $\left(\frac{\text{Normal force}}{qS}\right)$
C_Y	lateral-force coefficient $\left(\frac{\text{Lateral force}}{qS}\right)$
$\frac{dC_m}{d\alpha}$	rate of change of pitching-moment coefficient with angle of attack, per degree

$\frac{dC_n}{d\psi}$	rate of change of yawing-moment coefficient with angle of yaw, per degree
P	period of oscillation, seconds
I_y	moment of inertia about the Y-axis, slug-feet ²
I_z	moment of inertia about the Z-axis, slug-feet ²
\bar{c}	wing mean aerodynamic chord, feet
γ	flight-path angle, degrees

MODELS AND APPARATUS

The models are of all wooden construction with metal inserts bonded to the upper and lower surfaces of the wing and tail group. A three-view drawing of the model is presented as figure 1. The characterizing features of the design are a sweptback wing having inverse taper, a vee-tail arrangement set high on the fuselage, and a relatively short tail length. Pertinent areas and dimensions of the model components are given in table I. General views of the model are shown as figure 2.

The models are propelled by a standard 3.25-inch Mk. 7 aircraft rocket motor modified to incorporate a straight section at the minimum nozzle diameter. The purpose of this straight section is to move the motor farther forward in the model and thereby provide accommodation for the motor in the existing model geometry. This alteration has little effect on the motor specific impulse which is about 66 pound-second per pound.

Both models were launched from a zero-length launcher (fig. 3) set at an elevation angle of 60° for the B model and 75° for the C model. All control deflections and the wing and stabilizer incidences were set at 0°. As the B model was the first complete model of this series to be flown, it was considered advisable to secure a center-of-gravity position as far forward as possible to preclude any unforeseen trim changes that might lead to destructive accelerations. The consequent addition of ballast accounts for the comparatively low value of Mach number attained. The take-off weight was 50 pounds, the weight after the propellant was expended was 40.8 pounds, and the corresponding center-of-gravity locations, were, respectively, about 8 and 4 percent ahead of the leading edge of the mean aerodynamic chord. For the C model, the take-off weight was 47 pounds, the weight after propellant was expended was 37.8 pounds, and the center-of-gravity location was 4.48 percent of the mean aerodynamic chord for both conditions. The center of gravity was on the fuselage reference line for both models.

The data from the flight were obtained by the use of a two-channel telemeter housed in the nose section (fig. 4) and a Doppler velocimeter radar unit (fig. 5) located near the launching site. The telemeter for the B model was designed to give continuous signals to two ground stations of normal and lateral acceleration to an accuracy of ± 2 percent of full-scale deflection. The normal accelerometer failed to operate and the test was repeated using the C model. In this case, to insure satisfactory results, both telemeter channels were used to measure normal accelerations. Because the values of the forces to be measured were uncertain, normal accelerometers having two sensitivity ranges, $\pm 10g$ and $\pm 20g$, were used to insure instrumentation coverage in case of any unpredicted large trim changes.

Both models were tracked in flight by the radar unit to obtain the time history of the velocity along the flight path. The drag coefficients obtained from this velocity time history and from radiosonde records are accurate to ± 5 percent. The values of temperature and static pressure used in calculating density and speed of sound were obtained from radiosonde observations made at the time of firing. The variation of Reynolds number (based on the mean aerodynamic chord of 1.18 ft) with Mach number is presented in figure 6.

RESULTS AND DISCUSSION

Time histories of the flights of the two models are presented in figure 7. For the B model, data were obtained from the lateral accelerometer and the Doppler velocimeter for about 5 seconds of flight from take-off. For the C model, data were obtained from the normal accelerometers and the radar unit for about 6 seconds of flight from take-off. The maximum Mach numbers attained and the corresponding Reynolds numbers for the two flights are 1.01 and 8,600,000 for the B model and 1.07 and 8,700,000 for the C model. For the airplane, these Reynolds numbers would occur at about 50,000 feet altitude.

Lateral Force

Examination of figure 7(a) reveals an increase in lateral acceleration soon after take-off to a value close to $-3g$ at a Mach number of about 0.10. This acceleration persisted throughout most of the thrusting flight period, becoming 0 at $M = 0.99$ shortly before the propellant was expended and reaching a value of 0.8 at $M = 1.0$. As the possibilities of jet-misalignment effects obscuring the true nature of the data are always present during the powered portion of the flight, no attempt has been made herein to analyze any of the results in this region. Beyond the point at which the propellant was expended, the model went into a short-period damped oscillation, the lateral acceleration becoming 0 at

$M = 0.85$ ($t = 2.8$). It should be realized that the acceleration data are applicable only for the model wing loading, center-of-gravity location, and altitude. If a given force coefficient and Mach number are assumed, it can be shown that the acceleration developed becomes less as the wing loading and altitude are increased.

The values of lateral acceleration were converted to values of lateral-force coefficient by use of the relationship

$$C_Y = \frac{2Wa_y}{\rho V^2 S g}$$

and are shown plotted against Mach number in figure 8 for the coasting part of the flight. The values of the coefficient in the range of Mach numbers covered in the test ($M = 0.75$ to 1.0) are very small, being 0 from $M = 0.75$ to $M = 0.89$ then increasing to about 0.005 at $M = 1.0$.

Directional Stability

As indicated in reference 1, an approximate determination of the static-directional-stability parameter $\frac{dC_n}{d\psi}$ may be arrived at by the use of measured values of the period of the damped oscillation observed in the lateral-acceleration curve (fig. 7(a)) and the moment of inertia; thus,

$$\frac{dC_n}{d\psi} = \frac{4\pi^2 I_z}{57.3P^2 qS\bar{c}}$$

Application of this relationship produces a value of $\frac{dC_n}{d\psi}$ of approximately -0.002 at $M = 0.93$.

Normal Force

Examination of figure 7(b) reveals an increase in normal acceleration from take-off to a value of 6.7g at a Mach number of about 0.9. At this point, the acceleration decreases sharply, becoming 0 near $M = 1.0$ and continuing to a maximum negative value of about 6g at a Mach number of about 1.07 which corresponds to cessation of powered flight. Here the model went into a fairly short-period damped oscillation until 1.4 seconds after firing ($M = 0.98$) at which time the model again developed positive accelerations of about 3g. As the speed further decreased, the acceleration also decreased until at a Mach number of 0.79 the acceleration again went through 0, becoming slightly negative at $M = 0.76$.

The values of normal acceleration obtained from the flight test (fig. 7(b)) have been converted to values of normal-force coefficient by use of the relationship

$$C_N = \frac{2Wa_n}{\rho V^2 S g}$$

and are shown plotted against Mach number in figure 9 for the coasting portion of the flight. No abrupt trim change was experienced by the model until it attained a Mach number of 0.97. The magnitude of this trim change, for a center of gravity located at 4.48 percent mean aerodynamic chord, would amount to a change in normal-force coefficient of about 0.03. It is reasonable to assume (see reference 2) that at higher lift-coefficient values the Mach number at which this trim change occurs may be decreased.

Longitudinal Stability

Applying the general method of reference 1 (described in the section entitled "Directional Stability") to a short-period oscillation which appeared in the normal-acceleration curve of figure 7(b) coincident with the cessation of thrust ($t = 0.95$), approximate values of the static-longitudinal-stability parameter $\frac{dC_m}{d\alpha}$ have been computed and are presented in figure 10 plotted against Mach number. It can be seen that the model is statically stable. By assuming a lift-curve slope of 0.05, the neutral point can be calculated to fall at 45 percent of the mean aerodynamic chord.

Drag

The values of drag coefficient obtained from the model deceleration along the flight path after the propellant was expended were determined from the relationship

$$C_D = \frac{2W(a - g \sin \gamma)}{\rho g S V^2}$$

For the B model, the values of γ were determined from a refined flight-path analysis by assuming zero lift and by utilizing the known values of velocity, deceleration, and drag. As the C model was launched nearly vertically ($\gamma = 75^\circ$) no attempt was made to account for the component of gravity due to inclination of the flight path. The drag-coefficient values for this model were obtained over a lift-coefficient range of ± 0.02 . The drag data obtained from tests of both models are presented in figure 11 for comparison. Of general interest is the delayed drag rise which can be attributed to the ability of the sweptback wing to reduce the effects

of compressibility. No sharp force break is noted. The values of the drag coefficient, although somewhat lower than was anticipated from examination of other comparable high-speed configurations, are believed to be correct. For example, reference 3 gives a drag coefficient at $M = 0.8$ of 0.015 for a low-wing D-558 arrangement employing nearly the same wing-leading-edge and 50-percent-chord sweepback as the flight model. By taking into account the fuselage nose shape, the midwing location, and the high test Reynolds number of the flight model, the low value of drag coefficient produced can be readily accounted for. Comparison of the curves reveals very good agreement between the drag data of both flights, the C-model results extending the drag curve beyond $M = 1.0$. The highest value of the drag coefficient for the range of Mach number tested occurred at $M = 1.01$ and was equal to 0.044. It is noted that the drag coefficient appears to decrease somewhat for speeds above a Mach number of 1.0. It is felt that additional tests to higher speeds would be required to establish this point definitely.

CONCLUDING REMARKS

Data from flight investigations of two rocket-powered models representative of a fighter-type airplane configuration incorporating an inverse-taper wing and a vee tail gave the following indications concerning the variation of stability and drag for Mach numbers up to 1.07.

1. No unusual variation was exhibited in the lateral acceleration, the lateral oscillation quickly damping to zero.
2. The model experienced no abrupt trim change at low lift coefficients until it attained a Mach number of 0.97. At higher lift coefficients the Mach number at which this trim change occurs may be decreased.
3. The model was statically stable with the center of gravity located at 4.48 percent mean aerodynamic chord. By assuming a lift-curve slope of 0.05, the neutral point of the model at slightly supersonic Mach numbers was estimated to fall at approximately 45 percent of the mean aerodynamic chord.
4. An approximate analysis of oscillation data revealed a value of the static-directional-stability parameter $\frac{dC_n}{d\psi} = -0.002$ for the model at a Mach number of about 0.93.

5. The highest value of drag coefficient was equal to 0.044 and occurred at a Mach number of 1.01.

Langley Aeronautical Laboratory
National Advisory Committee for Aeronautics
Langley Field, Va.

REFERENCES

1. Bishop, Robert C., and Lomax, Harvard: A Simplified Method for Determining from Flight Data the Rate of Change of Yawing-Moment Coefficient with Sideslip. NACA TN No. 1076, 1946.
2. Mattson, Axel T., and Loving, Donald L.: Force, Static Longitudinal Stability, and Control Characteristics of a $\frac{1}{16}$ -Scale Model of the Bell XS-1 Transonic Research Airplane at High Mach Numbers. NACA RM No. L8A12, 1948.
3. Wright, John B., and Loving, Donald L.: High-Speed Wind-Tunnel Tests of a 1/16-Scale Model of the D-558 Research Airplane. Lift and Drag Characteristics of the D-558-1 and Various Wing and Tail Configurations. NACA RM No. L6J09, 1946.

TABLE I

ROCKET-POWERED MODEL CHARACTERISTICS

Item	True dimensions	Remarks
Fuselage:		
Over-all length, in.	62.00	
Maximum width, in.	6.00	At station 24.33
Maximum fuselage height, in.	8.20	At station 24.33
Frontal area, sq in.	40.70	Fuselage alone
Maximum height, in.	9.55	Including canopy (Station 15.54)
Maximum frontal area, sq in.	46.20	Including canopy
Finesness ratio	10.34	Based on maximum width
Wing:		
Theoretical root airfoil		Republic R-4, 40-1, 10-1.0 (normal to plan reference line) reduced leading edge
Theoretical tip airfoil		Republic R-4, 40-10-1.0 (normal to plan reference line) normal leading edge
Angle of incidence, deg	0	
Dihedral angle, deg	0	
Wing twist, deg	0	
Sweepback at 50 percent chord, deg	40	
Aspect ratio	3.07	
Taper ratio (inverse)	1:1.63	
Airfoil thickness ratio, percent	7.56	Parallel to plane of symmetry
Theoretical root chord, in.	10.56	Parallel to plane of symmetry
Theoretical tip chord, in.	17.17	Parallel to plane of symmetry
Chord at wing-fuselage intersection, in.	11.50	Parallel to plane of symmetry
Mean aerodynamic chord, in.	14.12	Located at station 27.84
Spanwise location of mean aerodynamic chord, in.	11.27	Measured normal to model center line
Vertical location of mean aerodynamic chord, in.	0.11	In reference to model center line
Total span, in.	41.78	Measured normal to model center line
Total wing area, sq in.	568	
Wing area enclosed by fuselage, sq in.	66.4	

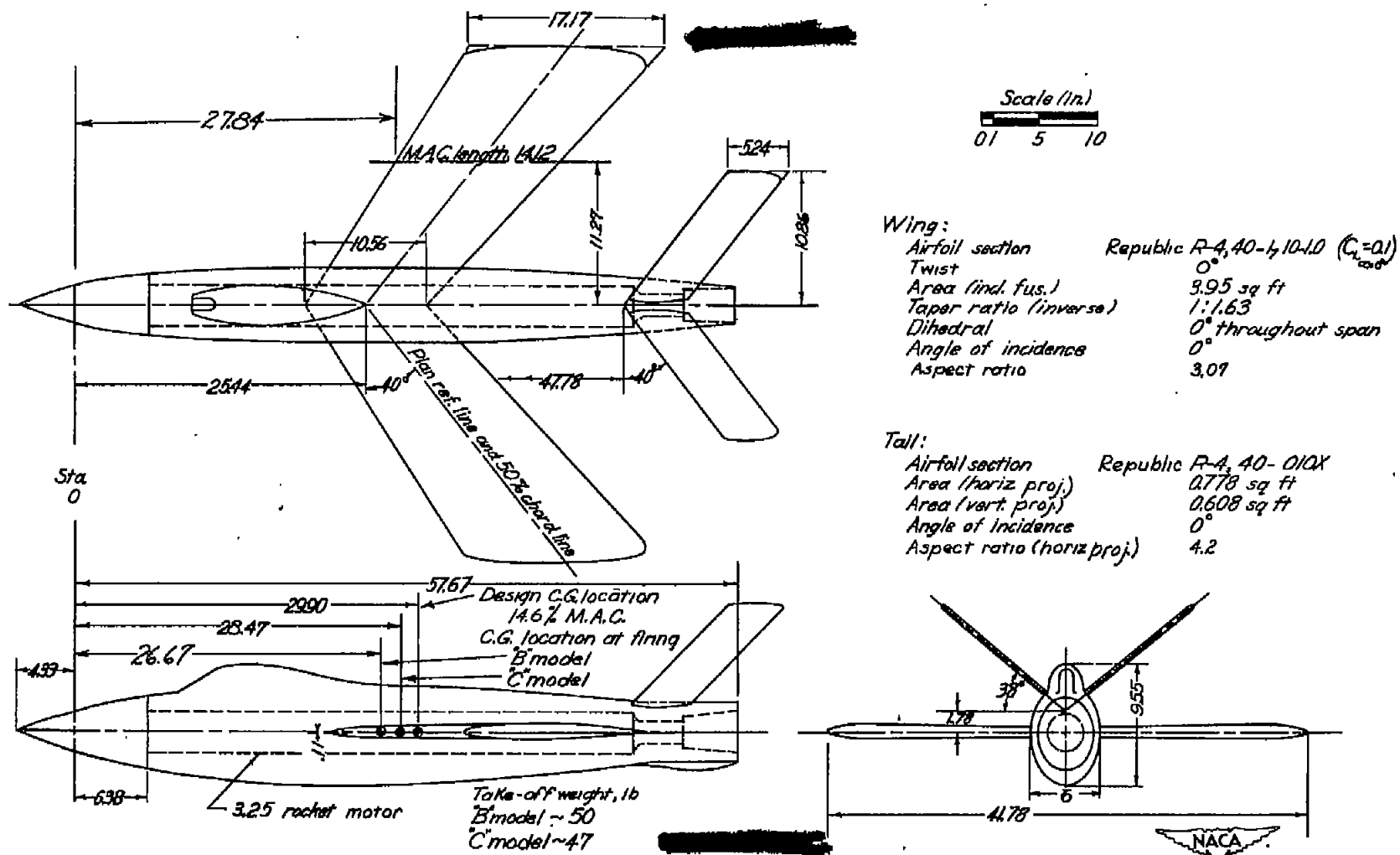
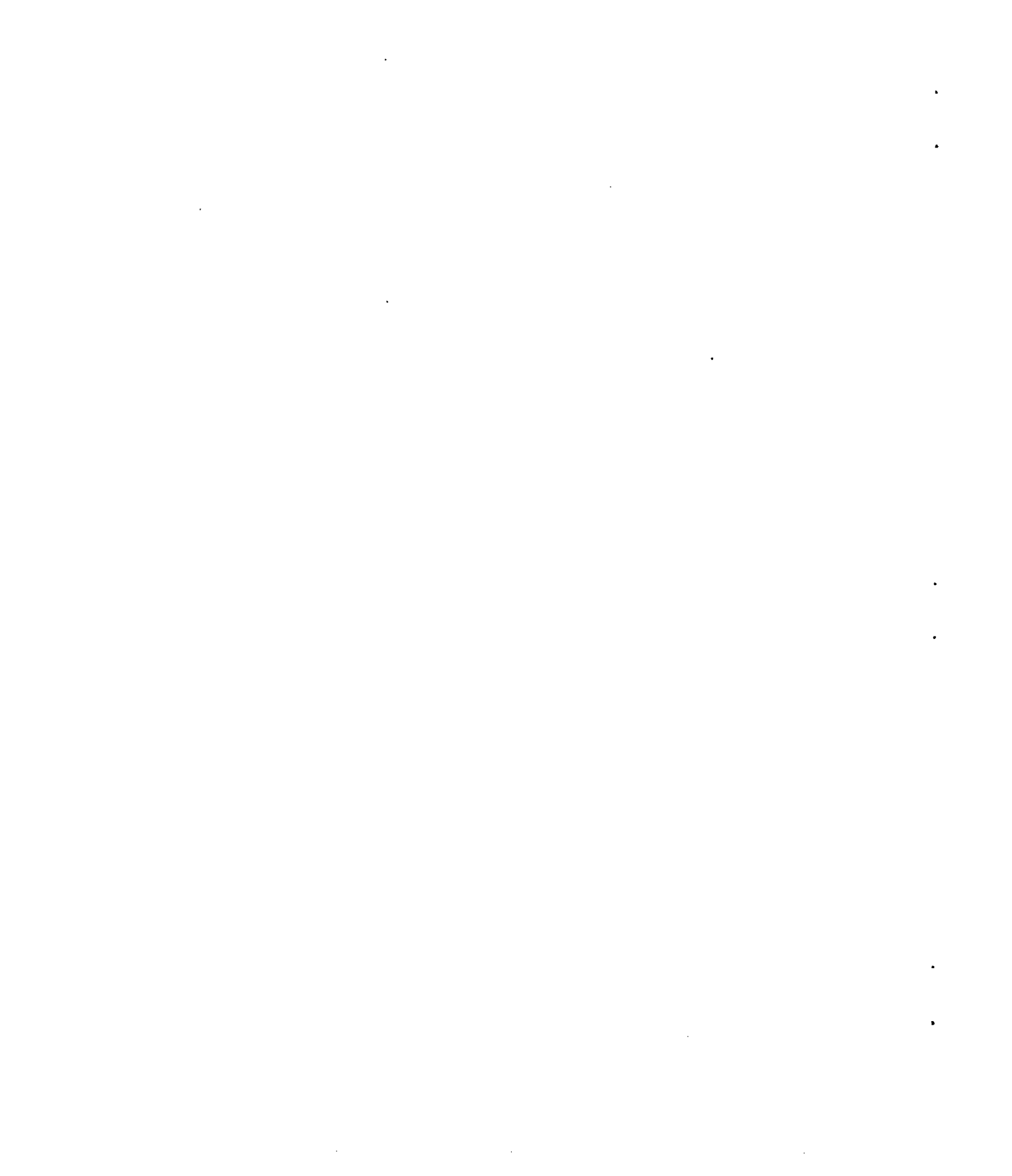
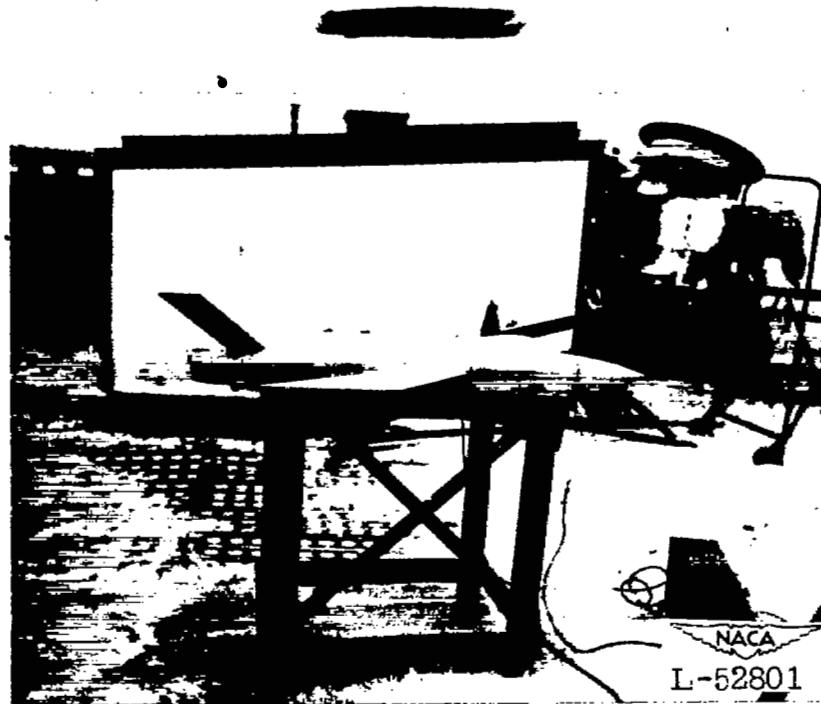
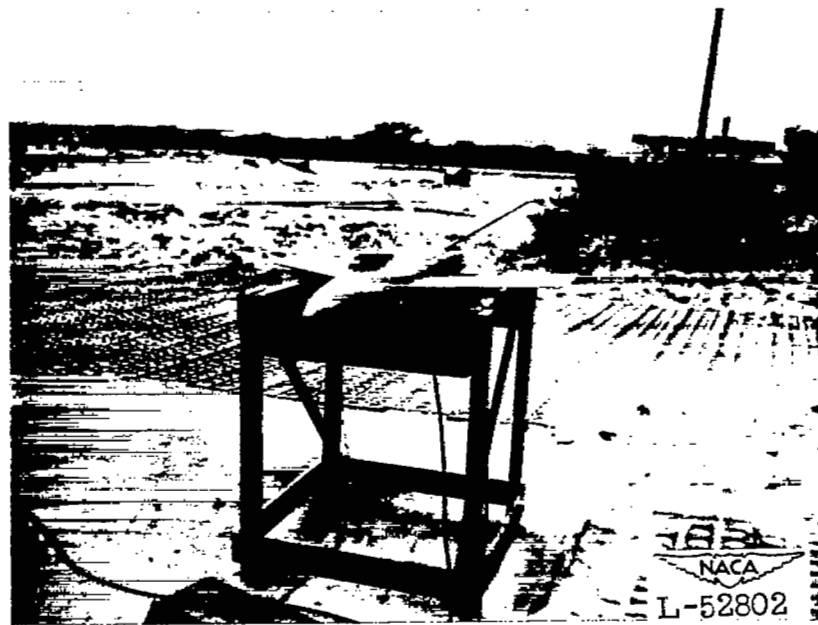


Figure 1.- General arrangement and dimensions of rocket-powered flight model. Controls undeflected; short tail length.





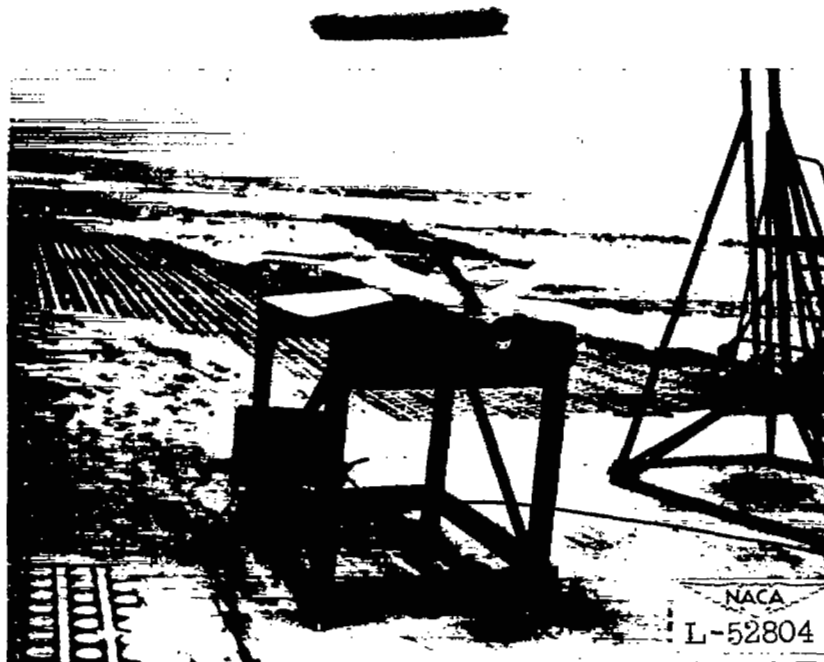
(a) Three-quarter front view.



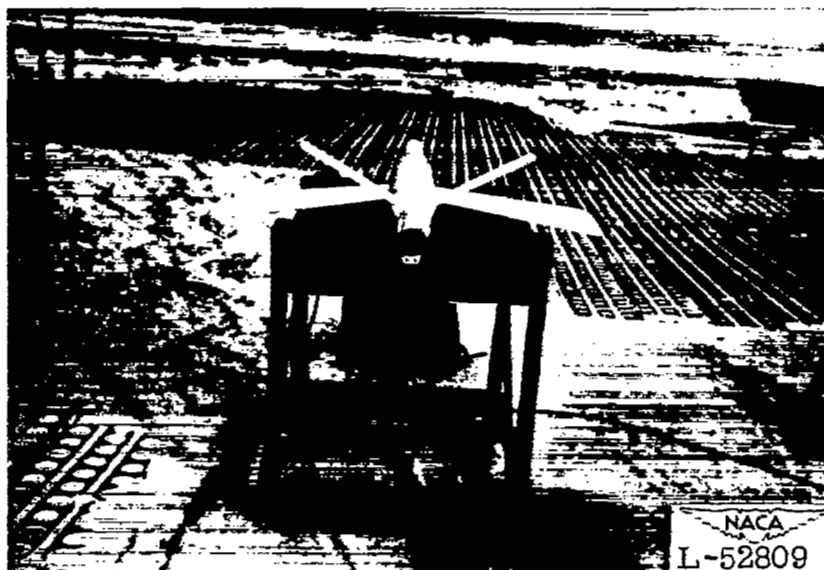
(b) Side view.

Figure 2.- General views of the model.





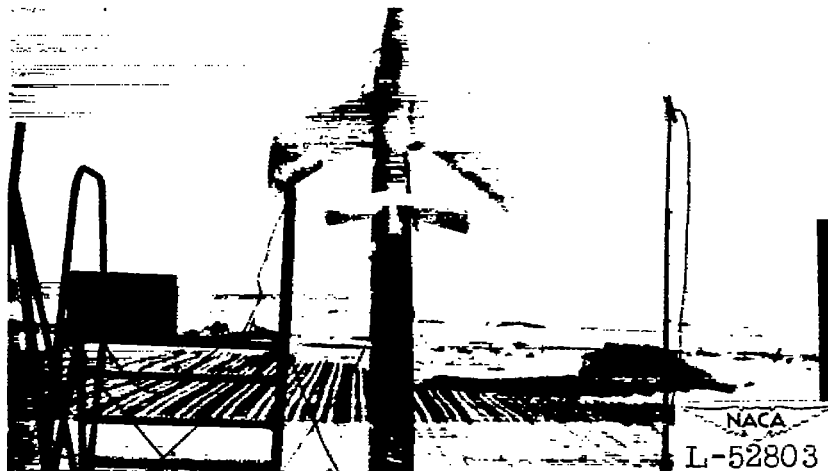
(c) Three-quarter rear view.



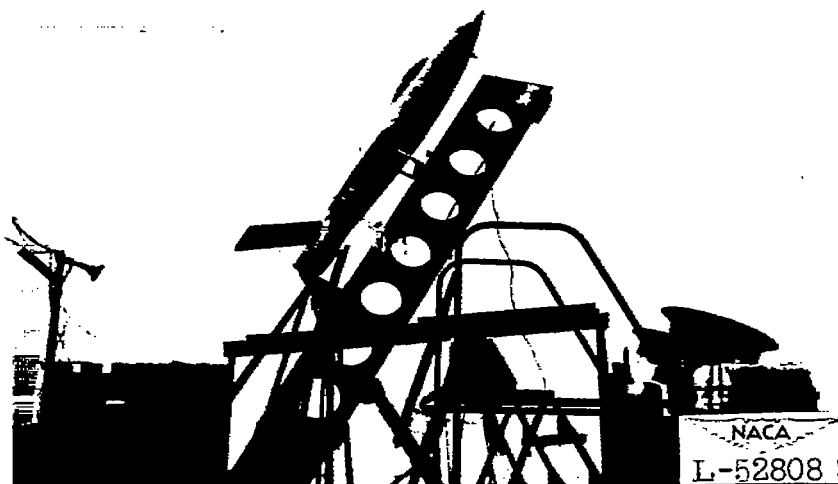
(d) Three-quarter top view.

Figure 2.- Concluded.





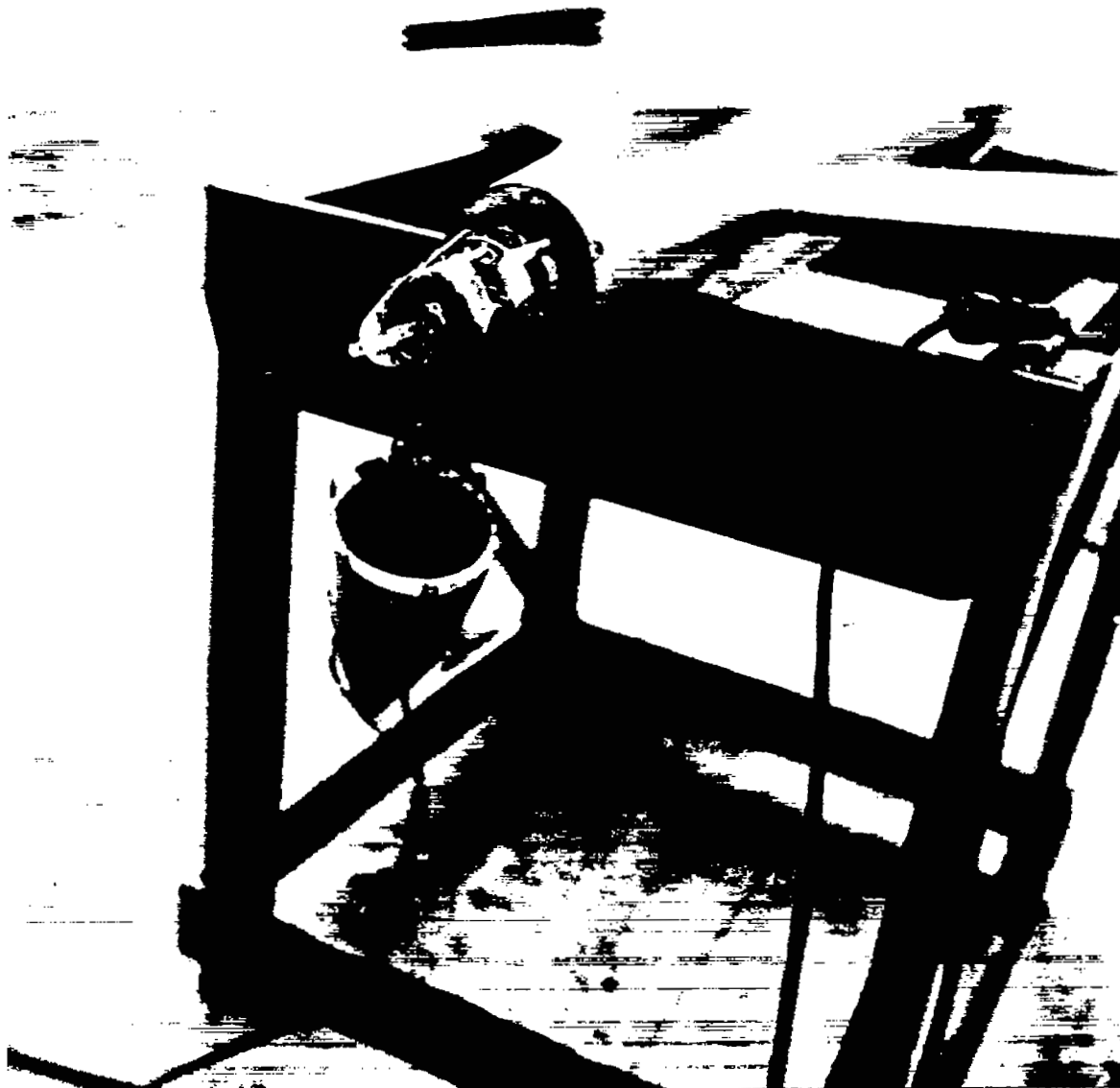
(a) Three-quarter top view.



(b) Side view.

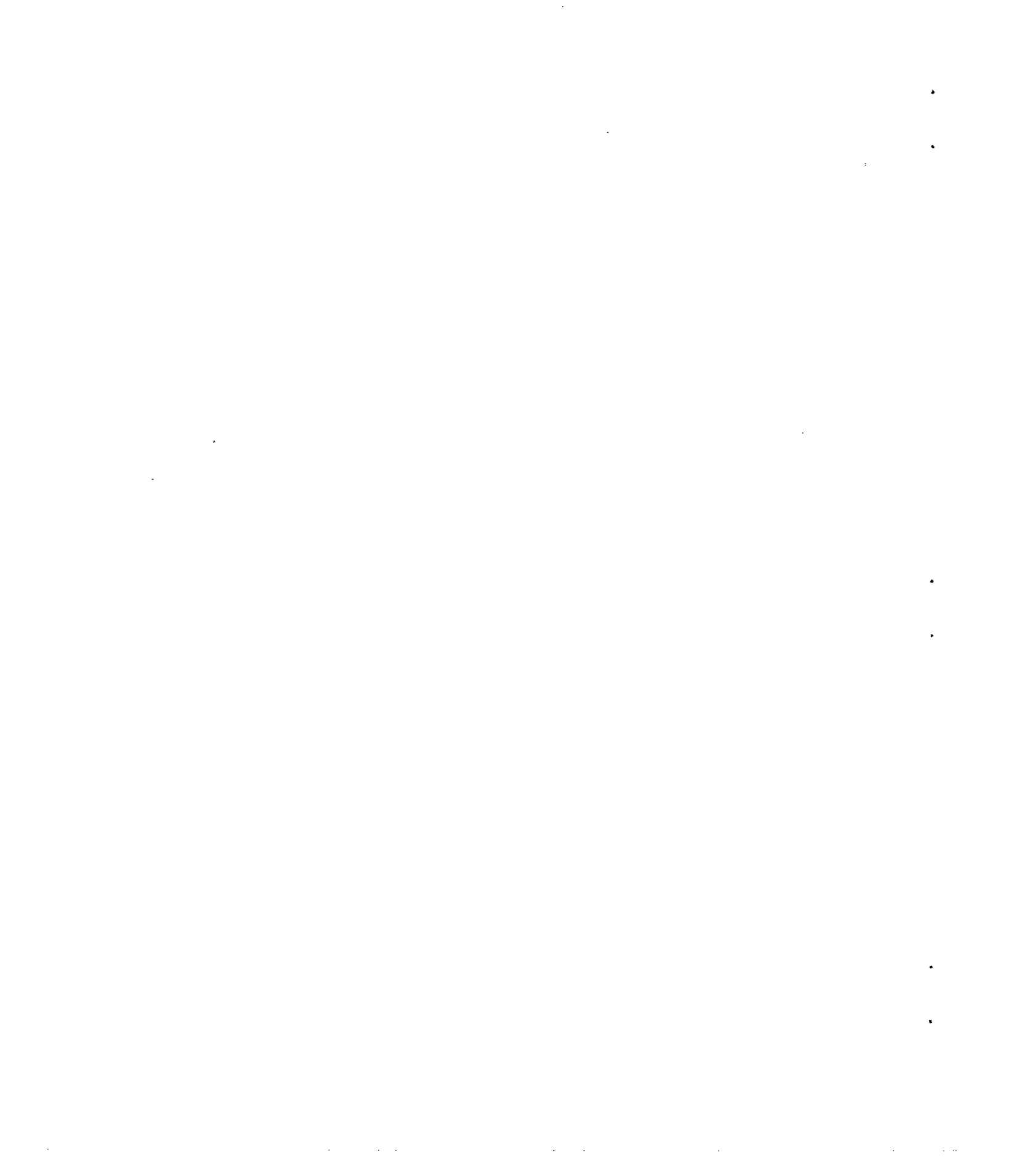
Figure 3.- Views of model on launcher.

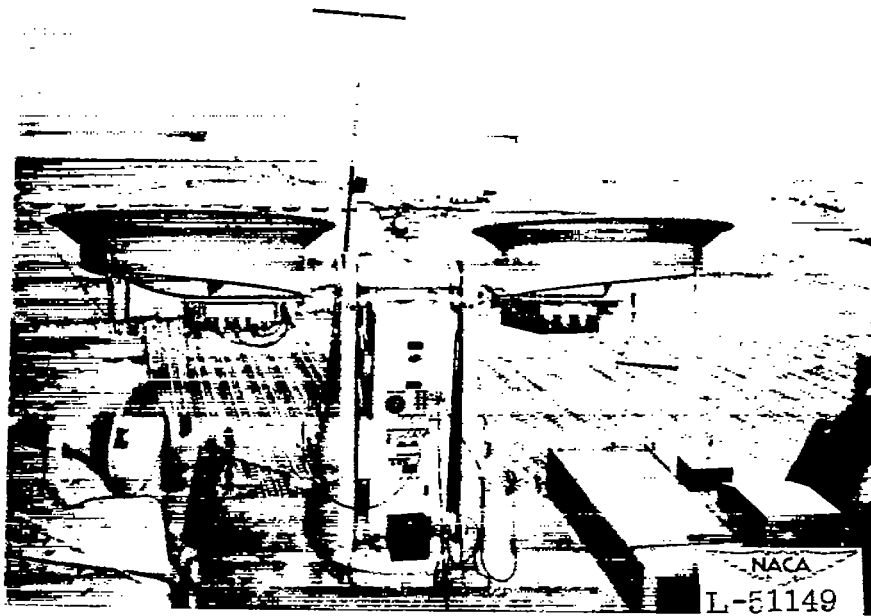




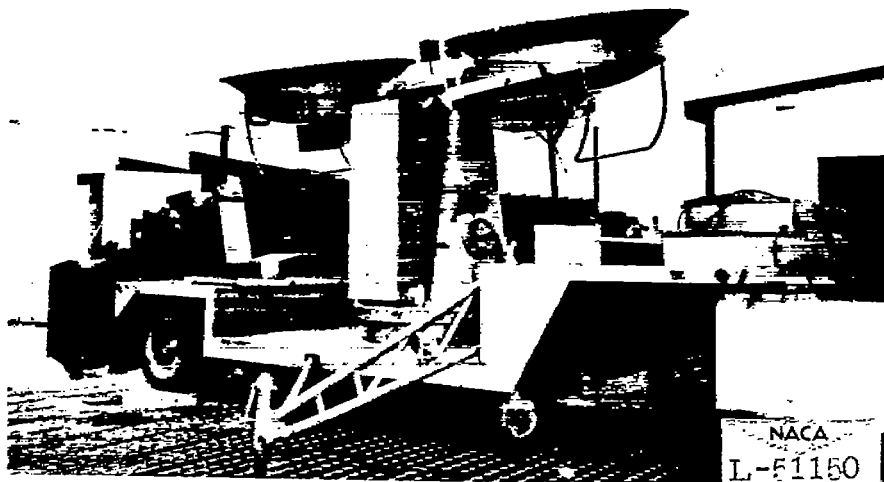
NACA
L-52812

Figure 4.- Two-channel telemeter installation for rocket-powered models.





(a) Three-quarter top rear view.



(b) Three-quarter front view.

Figure 5.- The Doppler velocimeter radar unit.



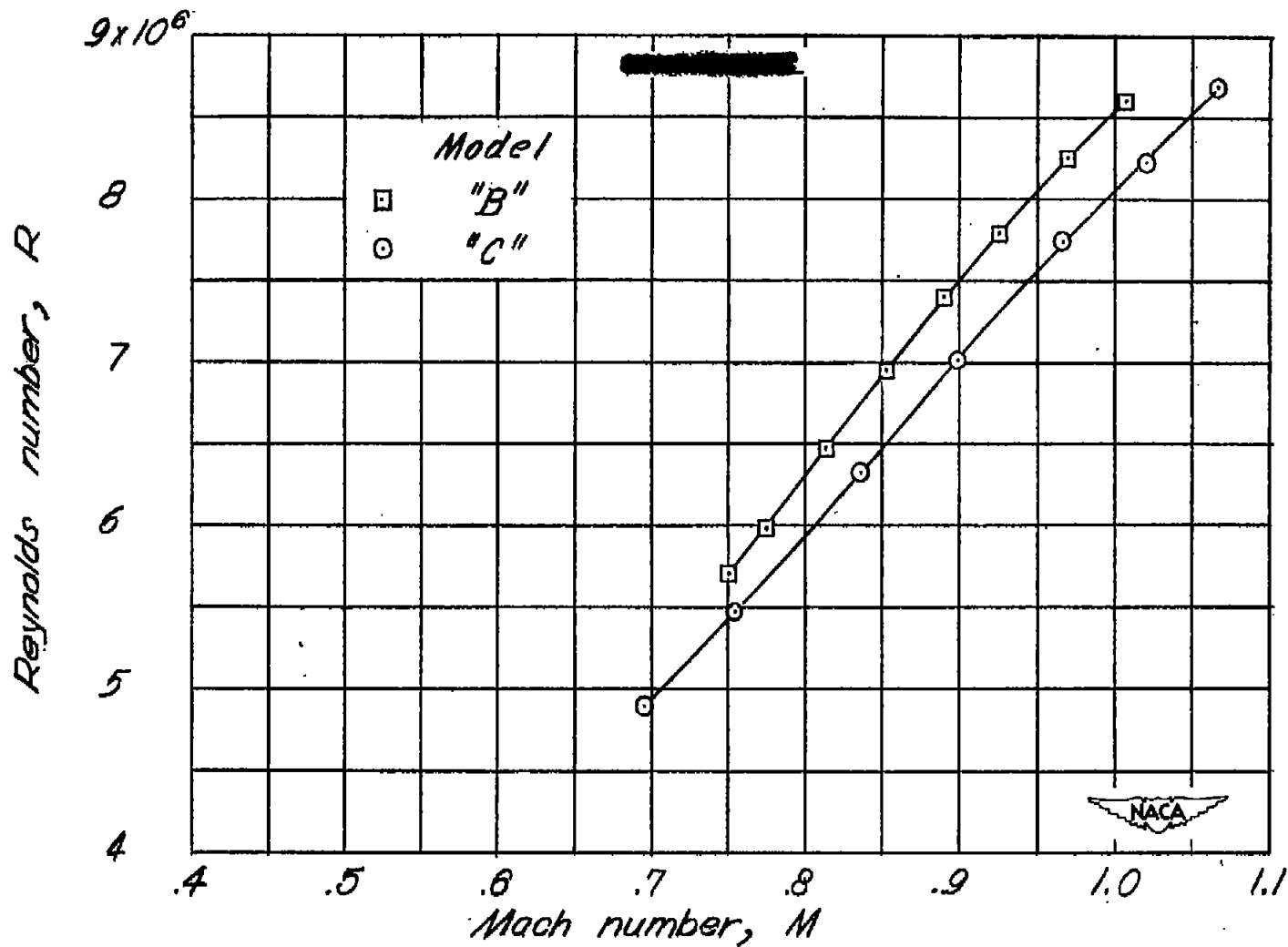
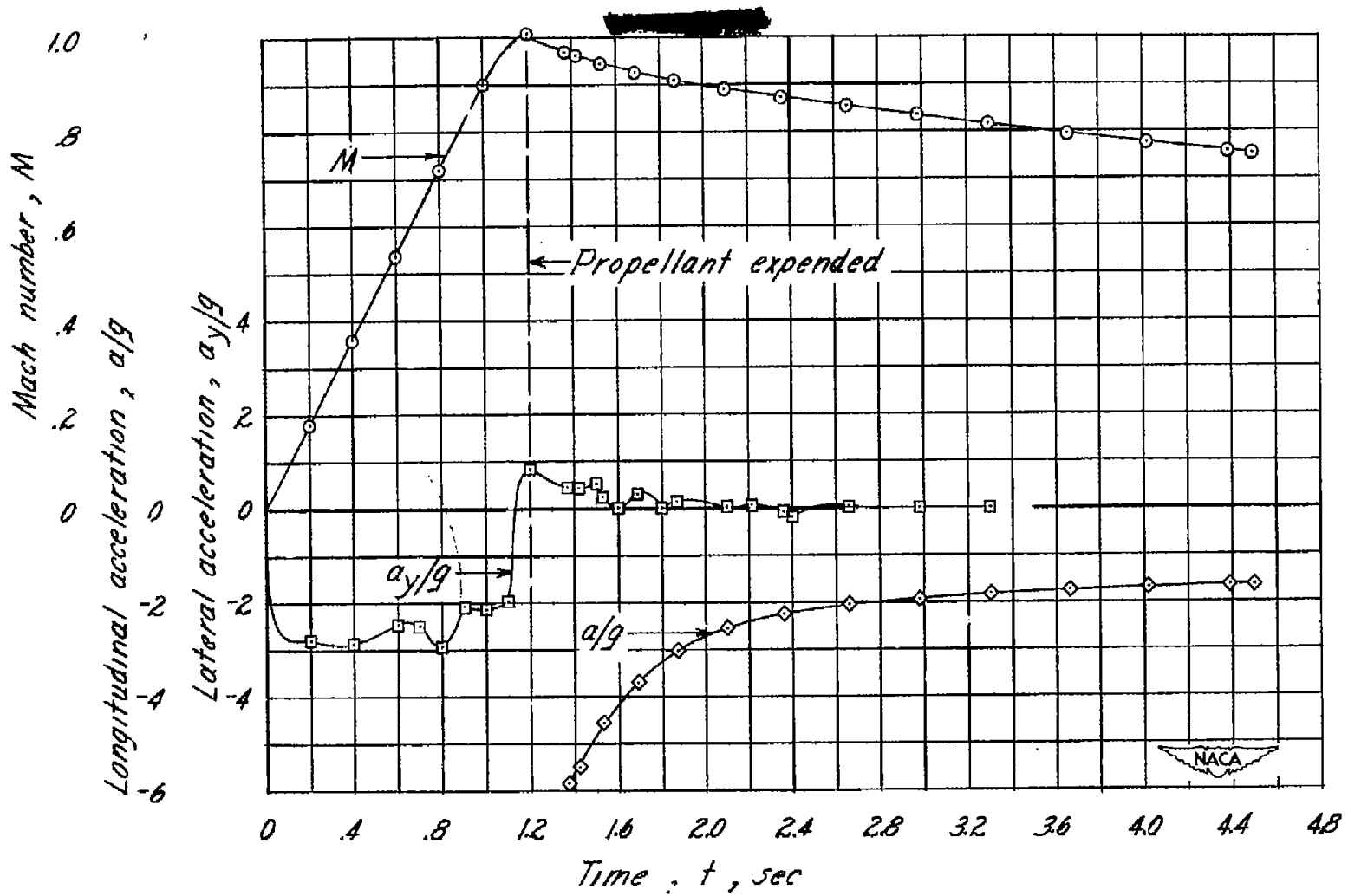
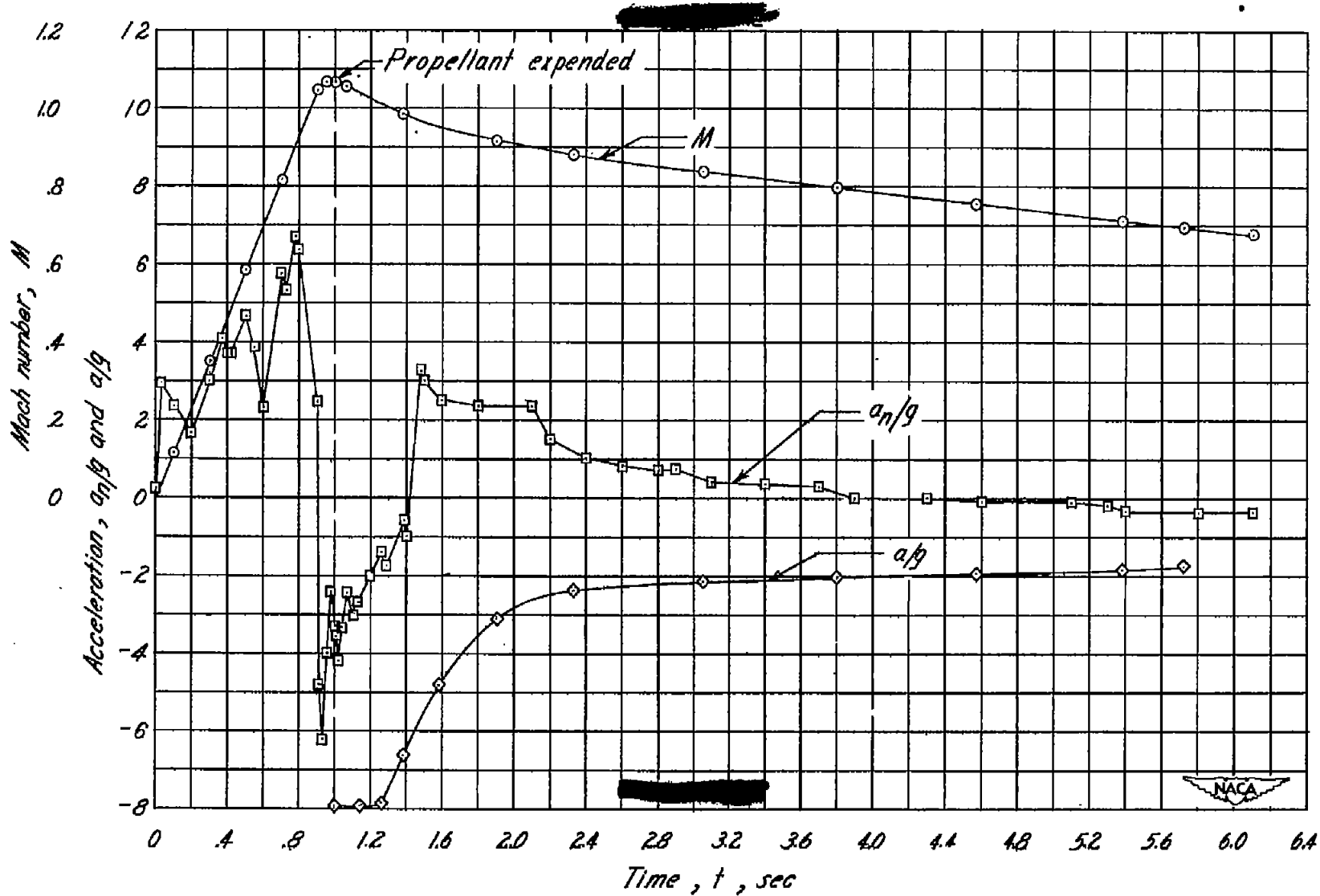


Figure 6.- Variation of Reynolds number with Mach number during coasting portion of flight.



(a) "B" model.

Figure 7. - Time history during flight period.



(b) "C" model.

Figure 7.- Concluded

Lateral-force coefficient, C_Y

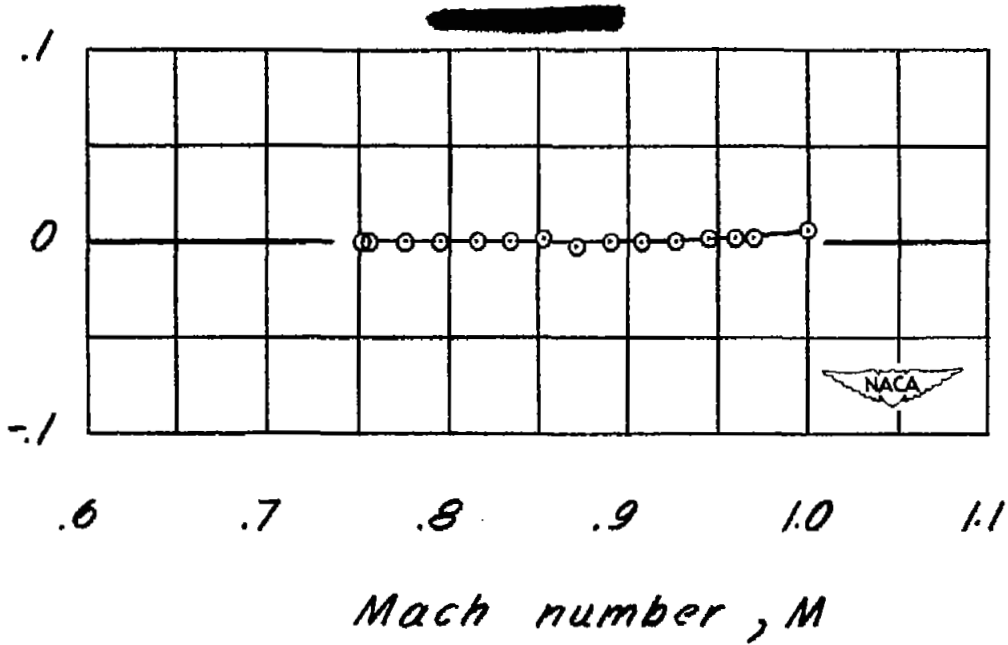


Figure 8.- Lateral-force characteristics during coasting portion of flight. Rocket-powered "B" model.

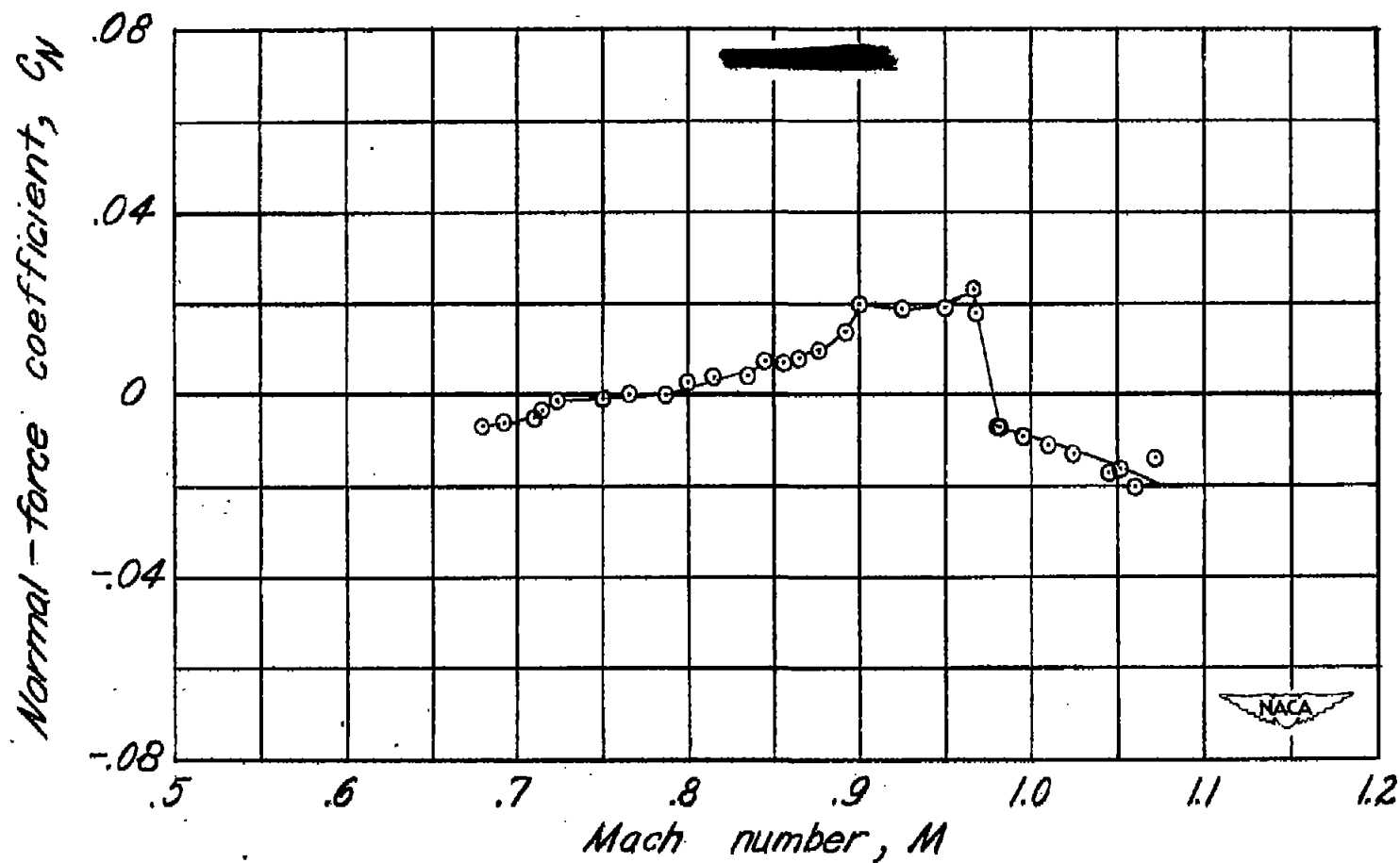


Figure 9.— Normal-force coefficient during coasting portion of flight. Rocket-powered "C" model. $W/S \cong 10$ lb/sq ft.

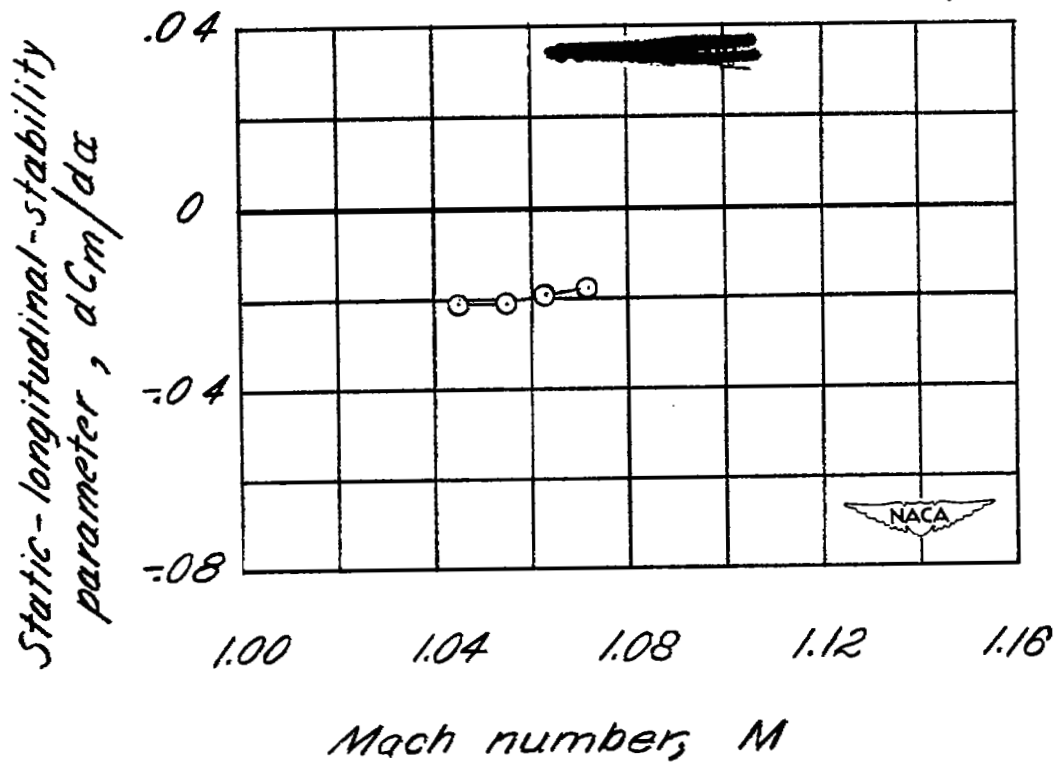


Figure 10. - Static longitudinal stability during coasting portion of flight. Rocket-powered "C" model.

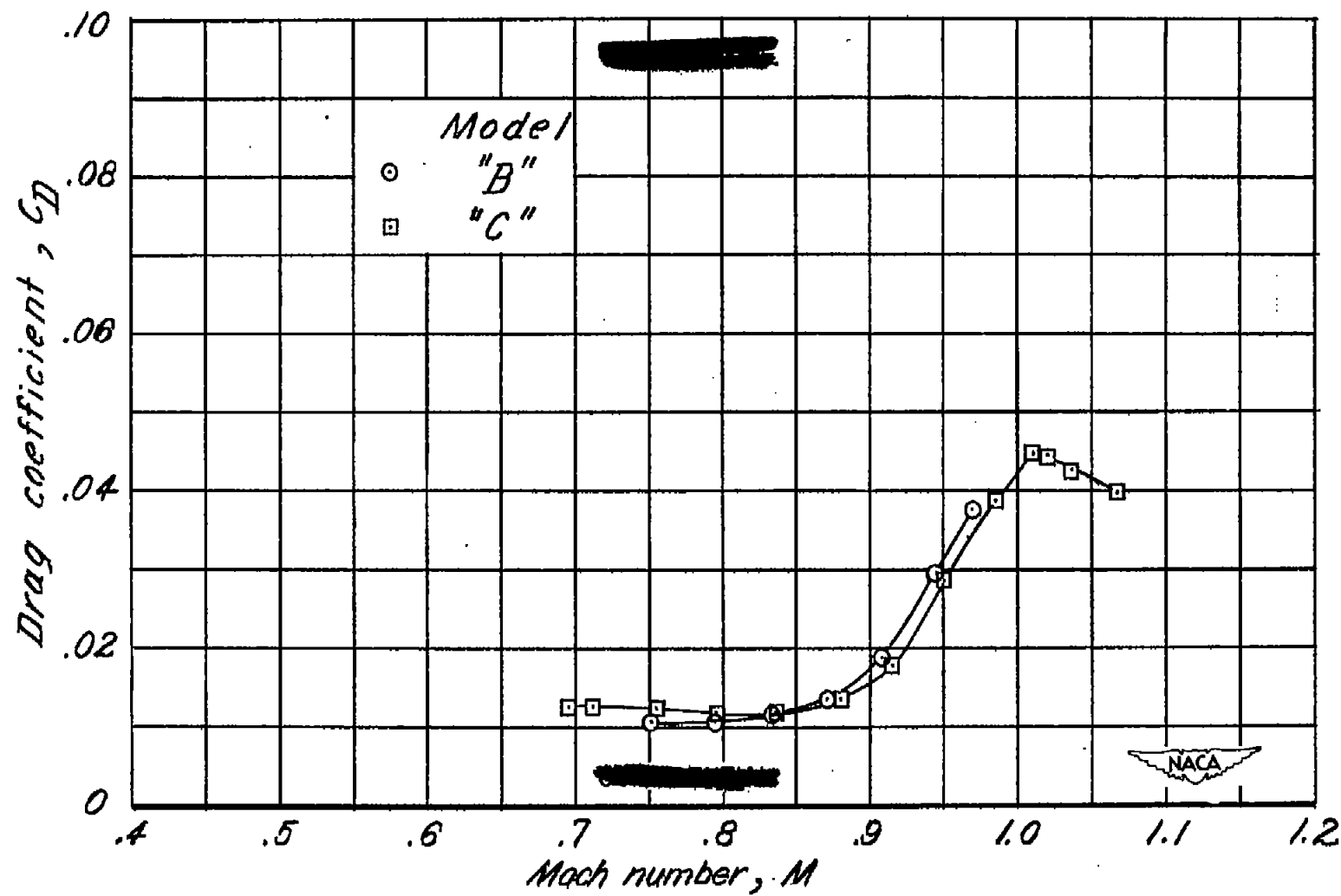


Figure 11.—Drag coefficients during coasting portion of flight.

LANGLEY RESEARCH CENTER



3 1176 01360 8329

DO NOT REMOVE SLIP FROM MATERIAL

Delete your name from this slip when returning material to the library.

NAME	DATE	MS
<i>Daniel Merri</i>	<i>11/3/97</i>	<i>153</i>

NASA Langley (Rev. Dec. 1991)

RIAD N-75